Effects of Oxidation on the Structure and Stability of Human Low-Density Lipoprotein†

Shobini Jayaraman,* Donald L. Gantz, and Olga Gursky

Department of Physiology and Biophysics, Boston University School of Medicine, Boston, Massachusetts 02118

Received February 2, 2007; Revised Manuscript Received March 13, 2007

ABSTRACT: Oxidation of low-density lipoprotein (LDL), the major cholesterol carrier in plasma, is thought to promote atherogenesis via several mechanisms. One proposed mechanism involves fusion of oxidized LDL in the arterial wall; another involves oxidation-induced amyloid formation by LDL apolipoprotein B. To test these mechanisms and to determine the effects of oxidation on the protein secondary structure and lipoprotein fusion *in vitro*, we analyzed LDL oxidized by nonenzymatic (Cu^{2+}, H_2O_2, and HOCl) or enzymatic methods (myeloperoxidase/H_2O_2/Cl^- and myeloperoxidase/H_2O_2/NO_2^-). Far-UV circular dichroism spectra showed that LDL oxidation induces partial unfolding of the secondary structure rather than folding into cross-β amyloid conformation. This unfolding correlates with increased negative charge of oxidized LDL and with a moderate increase in thioflavin T fluorescence that may result from electrostatic attraction between the cationic dye and electronegative LDL rather than from dye binding to amyloid. These and other spectroscopic studies of low- and high-density lipoproteins, which encompass amyloid-promoting conditions (high protein concentrations, high temperatures, acidic pH), demonstrate that *in vitro* lipoprotein oxidation does not induce amyloid formation. Surprisingly, turbidity, near-UV circular dichroism, and electron microscopic data demonstrate that advanced oxidation inhibits heat-induced LDL fusion that is characteristic of native lipoproteins. Such fusion inhibition may result from the accumulation of anionic lipids and lysophospholipids on the particle surface and/or from protein cross-linking upon advanced lipoprotein oxidation. Consequently, oxidation alone may prevent rather than promote LDL fusion, suggesting that additional factors, such as albumin-mediated removal of lipid peroxidation products and/or LDL binding to arterial proteoglycans, facilitate fusion of oxidized LDL *in vivo*.

Low-density lipoproteins (LDL[1]) mediate cholesterol delivery to peripheral tissues, and plasma levels of LDL, particularly of oxidized LDL (ox-LDL), correlate strongly with the progression of atherosclerosis (*1*−*3*). LDL comprise spherical particles of about 22 nm in diameter that contain an apolar core of cholesterol esters (CE) and triacylglycerols (TG) surrounded by an amphiphathic monolayer of phospholipids and unesterified cholesterol in which a single molecule of apolipoprotein B-100 (apoB, 4536 a.a.) is located. According to the "response to retention" hypothesis, LDL retention in the extracellular matrix of the arterial wall triggers a cascade of pro-atherogenic events, such as LDL oxidation, fusion, and lipid droplet formation, ultimately leading to foam cell formation and lipid deposition in atherosclerotic plaques (*4*, *5*).

LDL oxidation in plasma and, especially, in the arterial wall is thought to be a key pro-atherogenic event that leads to the formation of atherosclerotic lesions via multiple pathways ((*6*−*11*) and refs therein). One established pathway involves enhanced receptor-mediated uptake of ox-LDL by macrophages resulting in foam cell formation (*12*). Several mechanisms for such an enhanced uptake of ox-LDL have been proposed. According to one of them, fusion of ox-LDL increases their receptor-binding affinity and their retention in the arterial wall; such oxidation-induced LDL fusion *in vivo* is supported by multiple lines of circumstantial, albeit not direct, evidence (*13*). Another proposed mechanism suggests that amyloid formation by apoB on ox-LDL leads to enhanced uptake of ox-LDL by scavenger receptor CD36 that recognizes amyloid (*14*). Our work addresses these two putative mechanisms by testing whether LDL oxidation induces amyloid formation and particle fusion *in vitro*.

Advanced LDL oxidation results in apoB fragmentation, cross-linking, and increased solvent exposure (*6*, *15*), yet the secondary structure of apoB on ox-LDL is at least partially intact. Most CD and infrared studies of Cu^{2+}-oxidized LDL detect little or no secondary structural changes upon oxidation (*15*−*18*), and most of the observed changes involve partial unfolding of α-helix and/or β-sheet structure in apoB (*19*−*22*). Although LDL oxidation has been proposed to induce amyloid formation by apoB (*14*, *23*), little secondary structural evidence (*24*) supports oxidation-induced folding

† This work was supported by National Institutes of Health Grants GM067260 and HL026355.

* Corresponding author. Dr. Shobini Jayaraman, Department of Physiology and Biophysics, Boston University School of Medicine, W321, 715 Albany Street, Boston MA 02118. Tel: (617) 638-4247. Fax: (617) 638-4041. E-mail: shobini@bu.edu.

[1] Abbreviations: LDL, low-density lipoprotein; n-LDL, native (non-oxidized) low-density lipoprotein; ox-LDL, oxidized low-density lipoprotein; HDL, high-density lipoprotein; apoB, apolipoprotein B100; MPO, myeloperoxidase; CD, circular dichroism; ThT, thioflavin T; CE, cholesterol ester; TG, triacylglycerol; DTPA, diethylenetriamine pentaacetic acid; BHT, butylated hydroxytoluene; EDTA, ethylenediaminetetraacetic acid.

10.1021/bi700225a CCC: $37.00
Published on Web 04/20/2007

of apoB or its fragments in the cross-β-sheet conformation characteristic of amyloid.

One goal of this work was to test the amyloid hypothesis by carrying out CD spectroscopic analysis of LDL at advanced stages of oxidation when the protein structure is modified. To do so, we employed nonenzymatic agents that are widely used in LDL oxidation studies, such as Cu^{2+} ions, hydrogen peroxide (H_2O_2), and hypochlorite (HOCl), as well as myeloperoxidase, an oxidative enzyme that is expressed at high levels in atherosclerotic lesions and is believed to best represent LDL oxidation in the arterial wall (*8*). Another goal was to determine the effects of these oxidants on the heat-induced morphologic transitions in LDL. These thermal transitions in native (non-oxidized) LDL (n-LDL), which involve irreversible fusion into larger particles followed by particle rupture and apoB dissociation (*25*), were proposed to mimic *in vivo* LDL transformations such as fusion in the arterial wall. The current study tests whether LDL oxidation *in vitro* promotes heat-induced fusion; surprisingly, the results disprove both this notion and the amyloid hypothesis.

MATERIALS AND METHODS

Materials. Human myeloperoxidase (MPO) (lot # EC 1.11.1.7) was purchased from Calbiochem; MPO purity assessed by SDS gel electrophoresis was >95%, and the purity index A_{430}/A_{280} was 0.75. Thioflavin T (ThT) and $NaNO_2$ (99.99% purity) were from Sigma. Diethylenetriamine pentaacetic acid (DTPA, >98% purity) and NaOCl (<5% chlorine) were from Across Organic; the HOCl concentration was spectrophotometrically determined using extinction coefficient $\epsilon_{290} = 350\ M^{-1}\ cm^{-1}$ (*26*). The hydrogen peroxide (H_2O_2) 30% solution was from American Bioanalytical. Butylated hydroxytoluene (BHT, 99% purity) was from Aldrich.

LDL Isolation. Human LDL from five healthy volunteers were used in this work. Single-donor LDL were isolated from fresh EDTA-treated plasma by density gradient ultracentrifugation in the density range 1.019−1.063 g/mL (*27*). LDL migrated as a single band on agarose and SDS gels. Stock LDL solution of ∼4 mg/mL protein concentration was dialyzed extensively against buffer A (10 mM Na phosphate, 0.25 mM EDTA, and 0.02% NaN_3 at pH 7.5), degassed, and stored in the dark at 4 °C. The stock solution was used within two weeks during which no protein degradation and no changes in electrophoretic mobility of LDL were detected by SDS and agarose gel electrophoresis, respectively. Protein concentration was determined by modified Lowry assay.

LDL Oxidation and Characterization. LDL oxidation by nonenzymatic (Cu^{2+}, H_2O_2, and NaOCl) or enzymatic methods (MPO) was performed following established protocols. For copper oxidation, buffer B (10 mM Na phosphate at pH 7.5) was pretreated with washed Chelex resin (1 g/l) to remove traces of transition metals. LDL stock solution was dialyzed against buffer B for 18 h at 4 °C in the dark, using three buffer changes to remove traces of EDTA. Next, LDL solution of 0.1−4 mg/mL protein concentration was equilibrated at 37 °C, and oxidation was initiated by addition of $CuSO_4$ to 5 μM final concentration. The progress of lipid peroxidation measured by conjugated diene formation was monitored at 37 °C by absorbance at 234 nm using Varian Cary-300 UV/vis spectrometer with thermoelectric temperature control. Oxidation was stopped at different stages (marked 1−3 in Figure 1A) by addition of 1 mM EDTA and 10 μM BHT, followed by sample cooling on ice.

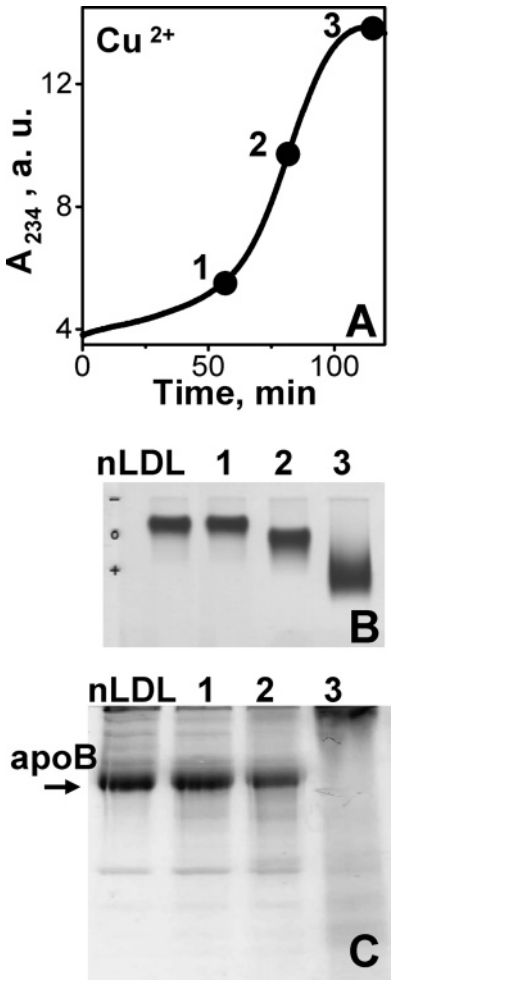

FIGURE 1: Copper-induced LDL oxidation and characterization. (A) Time course of LDL oxidation monitored by absorbance at 234 nm for conjugated diene formation. Oxidation of human LDL (0.1 mg/mL protein concentration in 10 mM Na phosphate buffer at pH 7.5) was initiated by addition of $CuSO_4$ (5 μM final concentration). Oxidation stages 1 (lag phase), 2 (propagation phase), and 3 (advanced phase) are indicated. (B) Effect of oxidation on the negative charge on LDL assessed by 1% agarose gel electrophoresis. Lanes 1−3 show the migration of LDL oxidized to stages 1−3, respectively (panel A). (C) Oxidation-induced protein modifications analyzed by 4% SDS gel electrophoresis. Lanes 1−3 show the migration of apoB oxidized to stages 1−3, respectively (panel A); n-LDL are shown for comparison.

The kinetics of Cu^{2+}-catalyzed oxidation is well characterized (*28*). During the lag phase (stage 1 in Figure 1A), antioxidants are consumed but only small amounts of lipid peroxidation products are formed; in the propagation phase (stage 2), poly unsaturated fatty acids in CE, TG, and phospholipids are progressively oxidized to lipid hydroperoxides; advanced oxidation (stage 3) corresponds to maximal concentration of aldehydes that can form Schiff bases with Lys residues of apoB. Agarose gel electrophoresis, which was used to monitor the progress of oxidation, showed gradual increase in LDL electronegativity in stages 2 and 3 (Figure 1B), reflecting Lys modifications in apoB and formation of free fatty acids. ApoB proteolysis during LDL oxidation, which results from nonenzymatic scission by aldehydes, was monitored by SDS gel electrophoresis (Figure

1C); as expected, stage 3 shows a continuous density streak, indicating apoB fragmentation, and large aggregates observed in stage 3 at the top of the gel are consistent with protein cross-linking by reactive aldehydes formed upon advanced oxidation ((*29*) and refs therein).

LDL oxidation by H_2O_2, which was triggered by the addition of 0.3% H_2O_2, was performed at 37 °C using a similar protocol. After the reaction reached an advanced stage, as judged by a plateau in absorbance at 234 nm, the LDL sample was dialyzed against buffer A to remove H_2O_2.

LDL oxidation by NaOCl was carried out as described (*30*). Briefly, freshly diluted NaOCl (0.5 mM) was added to the LDL sample (0.5 mg/mL protein concentration, 150 mM NaCl), and the sample was incubated for 2 h at 37 °C.

For MPO-induced oxidation, LDL solution of 0.2 mg/mL protein concentration in buffer A was first dialyzed against buffer C (50 mM Na phosphate buffer and 0.1 mM DTPA at pH 7.5). MPO/H_2O_2/Cl^--catalyzed oxidation was carried out with LDL solution in the presence of 150 mM NaCl. MPO was added to a final concentration of 3 nmol. Oxidation was initiated by addition of 40 μM H_2O_2 at 37 °C. The reaction was stopped by addition of 300 nM catalase followed by 30 min incubation at 25 °C (*31*).

MPO/H_2O_2/NO_2-oxidized LDL was prepared by incubating LDL (0.2 mg/mL protein concentration) at 37 °C in buffer C in the presence of 30 nM MPO and 0.5 mM $NaNO_2$ for 24 h. The reaction was terminated by adding 40 μM BHT and 300 nM catalase (*32*).

Gel Electrophoresis. SDS−polyacrylamide gel electrophoresis was performed using 4% homogeneous system. The gel was run at 150 V for 2 h and stained with Coomassie blue. Agarose gel electrophoresis was done using a TITAN gel lipoprotein electrophoresis system. LDL samples containing 4 μg of protein were loaded on the pre-cast gels, and the gels were run in barbital-sodium barbital buffer at 60 V for 40 min and at 125 V for 7 min. The gels were dried at 70 °C for 20 min, stained with 0.1% (w/v) Fat Red 7B stain in 95% methanol, destained in 75% methanol, and dried at 70 °C.

CD Spectropolarimetry and Turbidity. CD data were recorded using an AVIV-215 spectropolarimeter with a thermoelectric temperature controller. Heat-induced changes in CD and turbidity were recorded simultaneously at a constant wavelength (220 or 280 nm) as described (*33*). Far-UV CD spectra (185−125 nm) were recorded from LDL solutions of 0.1 mg/mL protein concentration. The CD and turbidity melting data were recorded from solutions of 2 mg/mL protein concentration during sample heating and cooling with 1 °C increment at a rate of 10 K/h. Far-UV CD data were normalized to protein concentration and expressed as molar residue ellipticity, [Θ]. ORIGIN software was used for data processing and display.

Fluorescence Spectroscopy. LDL (20 μg/mL) and ThT (8 μM) solutions in 10 mM Na phosphate buffer at pH 7.5, were mixed and incubated for 10 min. The emission spectra of ThT were recorded at 25 °C using a Fluoromax-2 spectrofluorimeter. The probe was excited at 450 nm, and the spectra were recorded from 460 to 600 nm with 5 nm excitation and emission slit widths.

Electron Microscopy. Lipoproteins were visualized by negative staining transmission electron microscopy as described (*25*) using a CM12 transmission electron microscope (Philips Electron Optics). Particle size analysis was carried out in PHOTOSHOP computer graphics using ~500 particles.

All experiments in this study were repeated at least five times to ensure reproducibility.

RESULTS

To determine the effect of LDL oxidation on the secondary structure in apoB, far-UV CD spectra were recorded of LDL that were extensively oxidized by various methods. To prepare such ox-LDL, n-LDL were incubated at 37 °C with various oxidants as described in Materials and Methods, and the time course of oxidation was monitored by UV absorbance at 234 nm. The peroxidation reached the advanced stage when the sigmoidal changes in absorbance reached a plateau (stage 3 in Figure 1A). Cu^{2+}-induced oxidation was stopped by addition of EDTA, while other nonenzymatic oxidative agents were removed by dialysis; the resulting ox-LDL were used for structural and stability studies.

Figure 2A shows far-UV CD spectra of n-LDL (solid line); consistent with earlier reports, these spectra have a maximum at 193 nm and a broad minimum from about 208 to 222 nm, indicating the presence of α-helix and β-sheet structure in apoB. The spectra of ox-LDL have similar shape but show reduced CD intensity at 208−222 nm, indicative of partial unfolding of the secondary structure. The rank order of the extent of this unfolding is HOCl, MPO/H_2O_2/Cl^- > H_2O_2, MPO/H_2O_2/NO_2^- > Cu^{2+} > n-LDL, with maximal unfolding (maximal reduction in CD intensity) induced by MPO/H_2O_2/Cl^- (▽) and minimal unfolding induced by Cu^{2+} (□). This reduction in CD intensity agrees with earlier CD studies (*19*, *22*) but is incompatible with amyloid formation because the latter would have led to a large increase (rather than reduction) in the negative CD near 217 nm, which is a hallmark of cross-β conformation ((*34*) and refs therein). Thus, contrary to the amyloid hypothesis, advanced oxidation of LDL by enzymatic as well as nonenzymatic methods leads to partial unfolding of the secondary structure in apoB rather than to folding in cross-β conformation.

To further test the amyloid hypothesis, we analyzed the effects of LDL oxidation on ThT binding/fluorescence. ThT is a benzothiazole dye that often exhibits large enhancement in fluorescence intensity upon binding to amyloid fibers. An increase in ThT emission was observed in the presence of ox-LDL and was interpreted as amyloid formation by apoB (*14*). However, ThT fluorescence alone does not provide a reliable tool for amyloid detection and should be correlated with structural data. In our studies, emission spectra of ThT were recorded in the presence of n-LDL or ox-LDL. In the presence of n-LDL, a ThT emission peak centered at 480 nm is observed (Figure 2B, black solid line). In the presence of Cu-oxidized as compared to n-LDL, this peak shows about 70% increase in amplitude (Figure 2B, □). A comparison of the fluorescence and CD spectra recorded from LDL that were oxidized to stage 3 by various agents (Figure 2A and B) shows a similar rank order for this fluorescence enhancement and for the extent of protein unfolding; thus, maximal fluorescence enhancement is induced by MPO/H_2O_2/Cl^- (▽), and minimal enhancement is induced by Cu^{2+} (□). This correlation between the increase in ThT fluorescence and

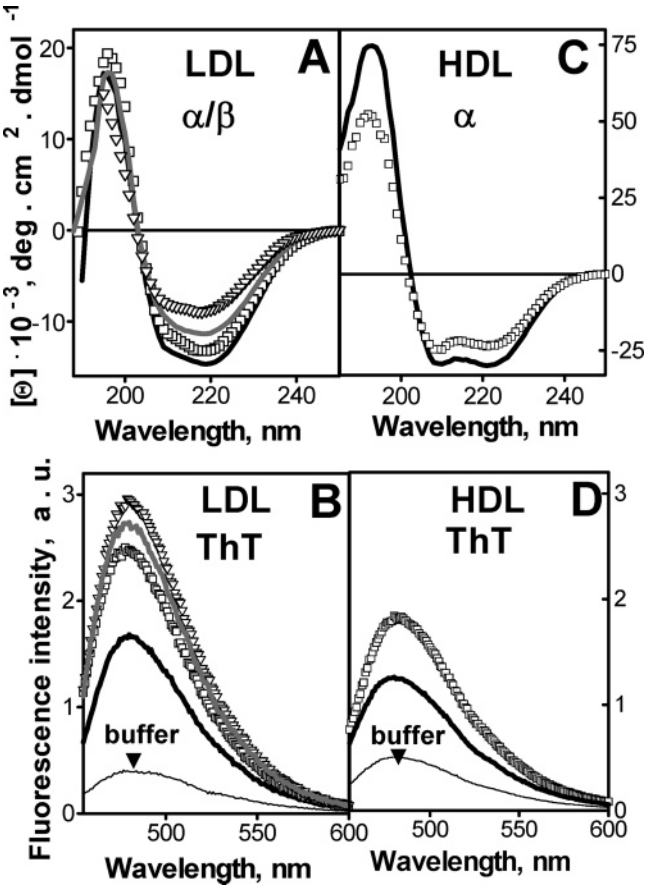

FIGURE 2: Effect of lipoprotein oxidation on the secondary structure and ThT binding. (A) Far-UV CD spectra of n-LDL (black solid line) and LDL oxidized to stage 3 by Cu^{2+} (□), MPO/H_2O_2/NO_2^- (gray line) and MPO/H_2O_2/Cl^- (▽). The spectra of LDL oxidized by using HOCl (which superimpose those using MPO/H_2O_2/Cl^- (gray line)) and by H_2O_2 (which superimpose those using MO/H_2O_2/NO_2^- (▽)) are not shown to avoid overlap. All spectra were recorded from LDL solutions of 0.1 mg/mL protein concentration in 5 mM Na phosphate buffer at pH 7.5 and 25 °C. (B) Fluorescence emission spectra of ThT at 25 °C in the presence of n-LDL or LDL oxidized to stage 3 by various agents. Line coding and buffer conditions are the same as those in panel A; the spectra of LDL oxidized by HOCl and by H_2O_2 are not shown to avoid overlap. LDL protein concentration is 0.02 mg/mL; ThT concentration is 8 μM. (C) Far-UV CD spectra of n-HDL (black line) and HDL oxidized to stage 3 by Cu^{2+} (□). Sample conditions are the same as those in panel A. (D) Fluorescence emission spectra of ThT in the presence of n-HDL and copper-oxidized HDL; sample conditions and line coding are the same as those in panel B.

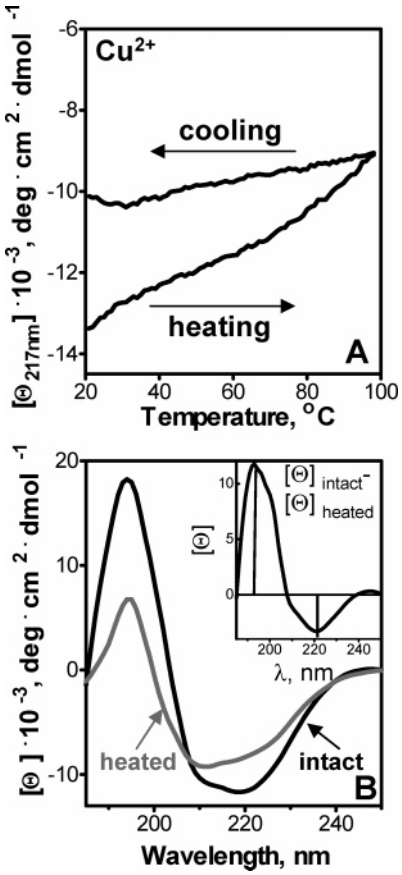

FIGURE 3: Effect of heating on the protein secondary structure in copper-oxidized LDL. LDL protein concentration is 40 μg/mL in 5 mM Na phosphate buffer at pH 7.5. (A) Secondary structure monitored by CD at 217 nm upon heating and cooling of ox-LDL at a rate of 11 K/h; the results closely resemble similar data for n-LDL (*25*). (B) Far-UV CD spectra of ox-LDL recorded at 25 °C before (black) and after heating to 98 °C (gray). (Inset) Difference spectrum between the intact and heated ox-LDL suggests irreversible heat-induced reduction in β-sheet content.

the extent of protein unfolding (rather than folding in cross-β conformation) implies that ThT fluorescence does not reflect amyloid formation by apoB. Furthermore, the increase in ThT fluorescence correlates directly with the increase in the electronegativity of ox-LDL as assessed by agarose gel electrophoresis, with the largest increase in electrophoretic mobility induced by MPO/H_2O_2/Cl^- (data not shown) and the smallest increase induced by Cu^{2+} (lane 3, Figure 1B). This suggests that the enhanced ThT fluorescence results, at least in part, from electrostatic attraction between the cationic dye and the negatively charged surface of ox-LDL.

To test whether the effects of oxidation on the apolipoprotein secondary structure and ThT fluorescence are specific to LDL, we carried out far-UV CD and ThT fluorescence studies of native human HDL (n-HDL) and HDL oxidized to stage 3 by Cu^{2+} (Figure 2C and D). In contrast to LDL, HDL are ~85% α-helical and lack substantial β-sheet structure that is thought to bind ThT. Nevertheless, HDL and LDL oxidation shows similar effects on the protein secondary structure and on ThT fluorescence: HDL oxidation by Cu^{2+} leads to partial unfolding of the helical structure indicated by far-UV CD (Figure 2C) and to an ~70% increase in the amplitude of ThT fluorescence, similar to that observed upon LDL oxidation (Figure 2B and D, □). Thus, regardless of the predominant secondary structure (α/β in LDL or α in HDL proteins), lipoprotein oxidation induces partial unfolding of this structure accompanied by a moderate increase in ThT fluorescence that may not reflect dye binding to cross-β conformation. Consequently, under conditions of our experiments, apoB on ox-LDL does not form amyloid.

Because amyloidogenic proteins often adopt cross-β conformation and readily form amyloid upon heating (*34*, *35*), we tested whether heating of ox-LDL may induce amyloid formation in apoB. The CD melting data $[\Theta_{220}](T)$ in Figure 3A, which were recorded at 220 nm upon slow heating and cooling of Cu-oxidized LDL from 5 to 98 °C, closely resemble similar data of n-LDL (*25*) and show a gradual reduction in the CD amplitude upon heating, suggesting non-cooperative partial unfolding of apoB. This is confirmed by far-UV CD spectra of ox-LDL recorded at

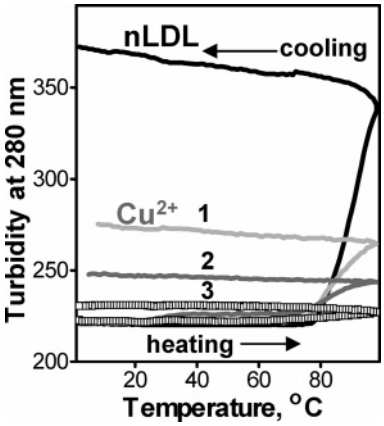

FIGURE 4: Effect of copper oxidation on thermal transition in LDL. The data were recorded by turbidity at 280 nm upon heating and cooling LDL solutions (2 mg/mL protein concentration and 10 mM Na phosphate buffer at pH 7.5) at a rate of 11 K/h. Melting data of n-LDL (black solid line) and LDL oxidized to stage 1 (light gray), stage 2 (dark gray), and stage 3 (□) (Figure 1) prior to heating are shown.

25 °C before and after heating to 98 °C (Figure 3B); the latter show not only reduced CD intensity but also altered spectral shape that indicates protein unfolding. The difference spectrum, $[\Theta]_{intact} - [\Theta]_{heated}$, shows a maximum at 195 nm and a minimum near 220 nm, which is characteristic of the β-sheet conformation (Figure 3B, insert). Consequently, heating of Cu^{2+}-oxidized LDL leads to a reduction in β-sheet content. Similar results were obtained using LDL oxidized by other agents (data not shown). Moreover, similar results were obtained under conditions that generally promote amyloid formation, such as acidic pH (pH 4.5−5.5) and high (4 mg/mL) protein concentrations. Thus, in contrast to the folding of the cross-β conformation observed in many amyloidogenic proteins at low pH, high temperatures, and/or high protein concentrations, heating of ox-LDL in a broad range of pH (pH 4.5−7.7) and protein concentrations (0.04−4 mg/mL) leads to β-sheet unfolding and hence does not produce amyloid.

Next, we tested the effect of oxidation on thermal stability and heat-induced fusion of LDL. Earlier, we showed that n-LDL undergo irreversible heat-induced transitions that involve the formation of smaller LDL-like particles ($\langle d \rangle$ = 20 nm) followed by lipoprotein fusion, rupture, and apoB dissociation (*25*). In the current work, we prepared LDL at stages 1−3 of Cu^{2+}-catalyzed oxidation (Figure 1) and monitored their thermal denaturation by measuring turbidity (dynode voltage) in CD experiments as described (*33*). LDL solutions of 2 mg/mL protein concentration were heated and cooled from 10 to 98 °C at a rate of 11 K/h, and turbidity at 280 nm, $V_{280}(T)$, was monitored as a function of temperature (Figure 4). The large irreversible increase in turbidity observed upon heating of n-LDL above 80 °C (Figure 4, black line) reflects lipoprotein fusion, rupture, and lipid coalescence into large droplets (*25*). Surprisingly, similar melting data recorded from LDL at various stages of oxidation show a progressive reduction in the amplitude of turbidity changes upon an increase in the degree of oxidation (Figure 4, lines 1−3). This suggests that oxidation by Cu^{2+} hampers heat-induced LDL fusion and rupture.

Similar results were obtained from LDL that were extensively oxidized by other agents. For example, Figure 5

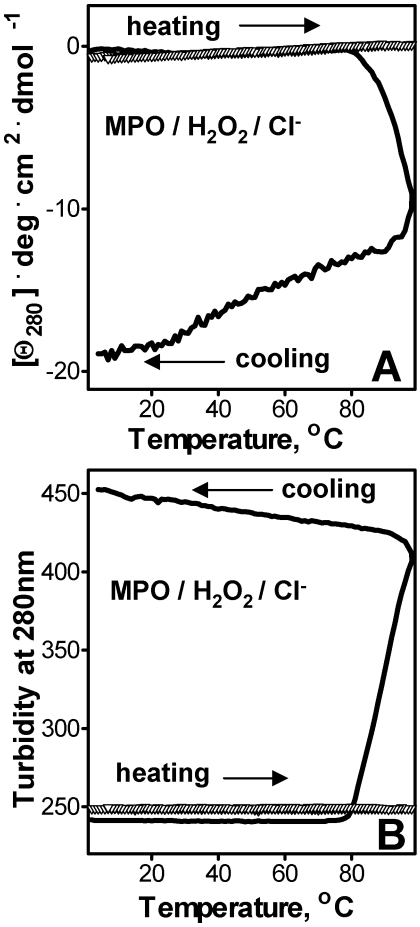

FIGURE 5: Effect of myeloperoxidase-induced oxidation on thermal transition in LDL. The CD (A) and turbidity (B) at 280 nm were recorded simultaneously during heating and cooling of n-LDL (black) or of LDL oxidized to stage 3 by $MPO/H_2O_2/Cl^-$ (▽). Experimental conditions are the same as those in Figure 4.

shows CD and turbidity melting data recorded at 280 nm of LDL oxidized to stage 3 by $MPO/H_2O_2/Cl^-$. The large irreversible increase in the negative CD at 280 nm observed in n-LDL upon heating above 80 °C is concomitant with the increase in turbidity (black lines in Figure 5A and B) and reflects re-packing of apolar core lipids during LDL rupture and coalescence into droplets (*25*). This heat-induced transition is completely abolished in LDL that have been oxidized to stage 3 by $MPO/H_2O_2/Cl^-$ (open symbols in Figure 5A and B) or other oxidative agents used in this study (data not shown). We conclude that advanced oxidation by various methods prevents heat-induced LDL fusion and rupture *in vitro*.

To further test this notion, ox-LDL were visualized by negative staining EM before and after heating to 98 °C. Figure 6 depicts the images of n-LDL and of LDL that were oxidized to stage 3 by Cu^{2+} prior to heating. EM data in Figure 6A and B show that oxidation induces no large changes in LDL size or morphology at ambient temperatures. Furthermore, our EM data reveal that LDL oxidation has a large effect on heat-induced changes in particle morphology. In contrast to n-LDL that undergo irreversible fusion, rupture, and lipid coalescence into droplets upon heating (Figure 6C), ox-LDL show no large heat-induced changes in morphology (Figure 6D). Furthermore, similar to Cu^{2+}-oxidized LDL, LDL that were oxidized to stage 3 by other methods remain

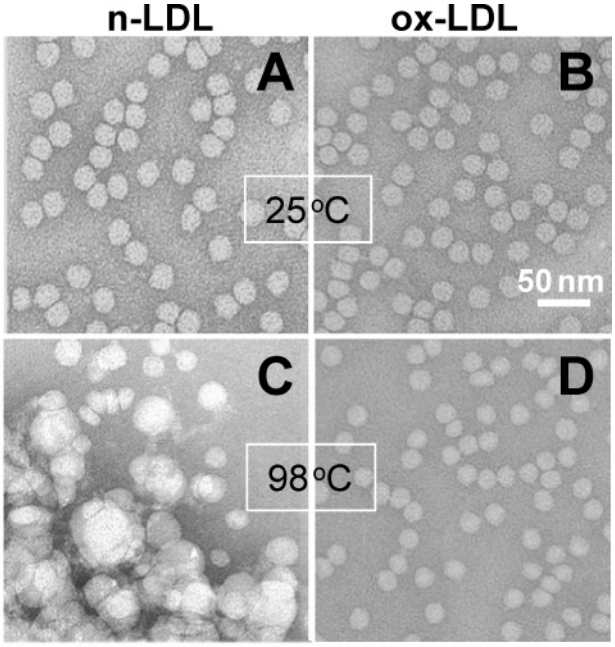

FIGURE 6: Effect of advanced oxidation on the heat-induced changes in LDL morphology. Electron micrographs of negatively stained n-LDL and LDL oxidized to stage 3 by Cu^{2+} were recorded at 25 °C before and after heating to 98 °C: n-LDL (A) and ox-LDL (B) before heating, and n-LDL (C) and ox-LDL (D) after heating. In contrast to n-LDL that show irreversible fusion, rupture, and lipid droplet formation upon heating to 98 °C, ox-LDL show only a small (~3 nm) reduction in the average particle diameter but no heat-induced fusion or rupture.

intact upon heating to 98 °C and show no large changes in size and morphology, as indicated by EM and native gel electrophoresis data (not shown). Importantly, EM images of ox-LDL do not show any fibrillar structures wider than 50 Å that could be interpreted as amyloid protofilaments (36), even though such structures are well within the resolution range of negative staining EM. These results, together with the turbidity and CD melting data in Figures 4 and 5, clearly show that advanced oxidation of LDL *in vitro* inhibits heat-induced particle fusion and disintegration and thereby stabilizes lipoprotein assembly.

DISCUSSION

The results of our spectroscopic studies clearly show that LDL oxidation *in vitro* does not induce cross-β-sheet conformation in apoB (Figures 2−5). We confirmed it by using six different oxidants in a broad range of conditions that include amyloid-promoting conditions, such as high (mg/mL) protein concentrations, high temperatures (98 °C), and acidic pH (pH 4.5−5.5). Thus, the moderate increase in ThT fluorescence observed in this and in the earlier studies of ox-LDL (*14*) must result from factors other than amyloid formation. One possibility is electrostatic attraction between cationic ThT and the LDL surface that becomes increasingly electronegative upon oxidation (Figure 1). In fact, electrostatic interactions have been proposed to be involved in interactions of ThT micelles with various macromolecular structures, including amyloid, keratin, and elastin fibrils, and DNA (*37*). The results of this (Figure 2B and D) and earlier studies (*14*) suggest that oxidized plasma lipoproteins such as HDL and LDL can be added to this list. Similarly, induced birefringence of Congo red upon binding to aggregates of ox-LDL (*14*) is not specific for amyloid and has been observed in many other protein systems, including collagen fibers, cytoskeletal proteins, and a wide variety of native and partially unfolded soluble proteins with diverse structures ((*38*) and refs therein). Similar to ThT binding, Congo red binding may have both electrostatic and hydrophobic components (*38*), which may contribute to enhanced interactions of these dyes with ox-LDL. Regardless of the exact origin of these interactions, our secondary structural data clearly show that apoB on ox-LDL does not form amyloid *in vitro*.

Similar to dye binding, the enhanced binding of serum amyloid P to ox-LDL reported in ref *14* is consistent with, but does not prove, amyloid formation. In fact, serum amyloid P binds not only to amyloid fibers but also to a wide variety of other ligands, including DNA, collagen, lipopolysachharides, phospholipids, normal HDL, and VLDL, apparently via a combination of Ca^{2+}-dependent electrostatic and hydrophobic interactions ((*39*, *40*) and refs therein). Furthermore, the low-angle X-ray diffraction of LDL reported in ref *14* may originate from ordering other than the cross-beta amyloid conformation. Thus, the diffuse 4.7 Å diffraction ring observed in n-LDL and in ox-LDL may originate from side-by-side packing of the lipid molecules, whereas a similar 9.8 Å ring that was detected only in ozone-oxidized LDL may be a high-order reflection from the lamellar ordering of CE and TG (~35 Å spacing) that occurs below physiologic temperatures in the particle core (*41*). In summary, the data in ref *14* can be explained by factors other than amyloid formation in ox-LDL.

Surprisingly, our turbidity, near-UV CD, and EM data in Figures 4−6 reveal that *in vitro* oxidation by various agents inhibits heat-induced LDL fusion, rupture, and apoB dissociation. Moreover, our ongoing studies suggest that this phenomenon is not limited to LDL but extends to other major classes of plasma lipoproteins. Earlier, we showed that heat- or denaturant-induced apolipoprotein dissociation is coupled to lipoprotein fusion that compensates for the decrease in the polar surface moiety (*25*, *42*, *43*). Now, we hypothesize that fusion inhibition in oxidized lipoproteins may result, in part, from protein cross-linking that prevents protein dissociation from the particle surface. However, such cross-linking occurs at advanced oxidation stages (stage 3, lane 3 in Figure 1C (*28*)), whereas gradual decrease in LDL fusion is detected at earlier stages of oxidation (lines 1−3 in Figure 4), suggesting that lipid peroxidation at these early stages may inhibit LDL fusion. In fact, free fatty acids and lysophospholipids, which form early upon the oxidation of the LDL surface, are expected to stabilize LDL and prevent fusion (*44*, *45*). Also, the peroxidation of CE and TG in the LDL core leads to the formation of free fatty acids and sterols and thereby increases the lipid core polarity; we propose that migration of these polar lipids from the LDL core to its surface increases the surface-to-core lipid ratio and thereby hampers lipoprotein fusion. In addition, accumulation of anionic lipids at the surface of ox-LDL would be expected to inhibit fusion because of increased spacial separation of lipid head groups within the particle. Finally, increased electrostatic repulsion between LDL particles whose net negative charge progressively increases upon oxidation (Figure 1B) may contribute to fusion inhibition. In summary, lipid peroxidation products and apolipoprotein cross-linking may potentially inhibit the fusion of ox-LDL.

The increased resistance of ox-LDL to heat-induced fusion observed in our work was surprising because the fusion of ox-LDL at ambient temperatures was reported in some, although not all, *in vitro* studies (*6*−*8*, *13*, *14*, *22*, *29*, *46*). Moreover, the linkage between LDL oxidation and fusion *in vivo* is supported by strong circumstantial evidence (*13*). The latter suggests that the factors mediating *in vivo* fusion of ox-LDL are absent from our *in vitro* experiments. For example, products of lipid peroxidation such as lysophospolipids and free fatty acids may stabilize LDL (*44*) and inhibit fusion (*45*); hence their removal by albumin may facilitate fusion of ox-LDL *in vivo*. Furthermore, LDL fusion, which is strongly concentration-dependent (*25*, *29*), may be aided by LDL accumulation upon binding to arterial proteoglycans (*13*, *47*).

In summary, the results reported here demonstrate that *in vitro* LDL oxidation does not lead to amyloid formation by apoB. We also show that, regardless of the oxidative agent, mere oxidation may inhibit rather than promote lipoprotein fusion. This suggests that *in vivo* fusion of ox-LDL in the arterial wall, which is proposed to trigger a cascade of proatherogenic events at early stages of atherosclerosis, is aided by other factors, such as LDL binding to arterial proteoglycans (*47*), interactions with albumin (*44*), and so forth. Identification of these fusion-promoting factors may potentially help develop new therapeutic targets for atherosclerosis.

ACKNOWLEDGMENT

We thank Cheryl England and Michael Gigliotti for help with lipoprotein isolation, and Drs. David Atkinson and Donald M. Small for valuable advice.

REFERENCES

1. Brown, M. S., and Goldstein, J. L. (1986) A receptor-mediated pathway for cholesterol homeostasis, *Science 232*, 43−47.
2. Holvoet, P., Vanhaecke, J., Janssens, J., Van de Werf, F., and Collen, D. (1998) Oxidized LDL and malondialdehyde-modified LDL in patients with acute coronary syndromes and stable coronary artery disease, *Circulation 98*, 1487−1494.
3. Ehara, S., Ueda, M., Nakuro, T., Haze, K., Itoh, A., Otsuka, M., Komatsu, R., Matsuo, T., Itabe, H., Takano, T., Tsukamoto, Y., Yoshiyama, M., Takeuchi, K., Yoshikawa, J., and Becker, A. E. (2001) Elevated levels of oxidized low density lipoprotein show a positive relationship with the severity of acute coronary syndromes, *Circulation 103*, 1955−1960.
4. Camejo, G., Hurt-Camejo, E., Wiklund, O., and Bondjers, G. (1998) Association of apo B lipoproteins with arterial proteoglycans: pathological significance and molecular basis, *Atherosclerosis 139*, 205−222.
5. Williams, K. J., and Tabas, I. (1998) The response-to-retention hypothesis of atherogenesis reinforced, *Curr. Opin. Lipidol. 9*, 471−474.
6. Jurgens, G., Hoff, H. F., Chisolm, G. M., and Esterbauer, H. (1987) Modification of human serum low-density lipoprotein by oxidation. Characterization and pathophysiological implications, *Chem. Phys. Lipids 45*, 315−336.
7. Steinberg, D., Partharasathy, S., Carew, T. E., Khoo, J. C., and Witztum, J. L. (1989) Beyond cholesterol. Modifications of low-density lipoprotein that increase its atherogenecity, *N. Engl. J. Med. 320*, 915−924.
8. Heinecke, J. W. (1997) Mechanisms of oxidative damage of low density lipoprotein in human atherosclerosis, *Curr. Opin. Lipidol. 8*, 268−274.
9. Witztum, J. L., and Steinberg, D. (2001) The oxidative modification hypothesis of atherosclerosis: does it hold for humans? *Trends Cardiovasc. Med. 11*, 93−102.
10. Navab, M., Ananthramaiah, G. M., Reddy, S. T., Van Lenten, B. J., Ansell, B. J., Fonarow, G. C., Vahabzadeh, K., Hama, S., Hough, G., Kamranpour, N., Berliner, J. A., Lusis, A. J., and Fogelman, A. M. (2004) The oxidation hypothesis of atherogenesis: the role of oxidized phospholipids and HDL, *J. Lipid Res. 45*, 993−1007.
11. Stocker, R., and Keaney, J. F., Jr. (2004) Role of oxidative modifications in atherosclerosis, *Physiol. Rev. 84*, 1381−1478.
12. Henricksen, T., Mahoney, T. M., and Steinberg, D. (1983) Enhanced macrophage degradation of biologically modified low-density lipoprotein, *Arteriosclerosis 3*, 149−159.
13. Oorni, K., Pentikainen, M. O., Ala-Korpela, M., and Kovanen, P. T. (2000) Aggregation, fusion, and vesicle formation of modified low density lipoprotein particles: molecular mechanisms and effects on matrix interactions, *J. Lipid Res. 41*, 1703−1714.
14. Stewart, C. R., Tseng, A. A., Mok, Y. F., Staples, M. K., Schiesser, C. H., Lawrence, L. J., Varghese, J. N., Moore, K. J., and Howlett, G. J. (2005) Oxidation of low-density lipoproteins induces amyloid-like structures that are recognized by macrophages, *Biochemistry 44*, 9108−9116.
15. Ettelaie, C., Haris, P. I., James, N. J., Wilbourn, B., Adam, J. M., and Bruckdorfer, K. R. (1997) Alterations in the structure of apolipoprotein B-100 determine the behavior of LDL towards thromboplastin, *Biochim. Biophys. Acta 1345*, 237−247.
16. Herzyk, E., Lee, D. C., Dunn, R. C., Bruckdorfer, K. R., and Chapman, D. (1987) Changes in the secondary structure of apolipoprotein B-100 after Cu^{2+}-catalysed oxidation of human low-density lipoproteins monitored by Fourier transform infrared spectroscopy, *Biochim. Biophys. Acta 922*, 145−154.
17. Vanderyse, L., Devreese, A. M., Baert, J., Vanloo, B., Luins, L., Ruysschaert, J. M., and Rosseneu, M. (1992) Structural and functional properties of apolipoprotein B in chemically modified low density lipoproteins, *Atherosclerosis 97*, 187−199.
18. Ursini, F., Davies, K. J. A., Maiorino, M., Parasassi, T., and Sevanian, A. (2002) Atherosclerosis: another protein misfolding disease? *Trends Mol. Med. 8*, 370−374.
19. McLean, L. R., and Hagaman, K. A. (1989) Effect of probucol on the physical properties of low-density lipoproteins oxidized by copper, *Biochemistry 28*, 321−327.
20. Brunelli, R., Mei, C., Krasnowska, E. K., Pierucci, F., Zichella, L., Ursini, F., and Parasassi, T. (2000) Estradiol enhances the resistance of LDL to oxidation by stabilizing apoB-100 conformation, *Biochemistry 39*, 13897−13903.
21. Chehin, R., Rengel, D., Milicua, J. C. G., Goni, F. M., Arrondo, J. L. R., and Pifat, G. (2000) Early stages of LDL oxidation: apolipoprotein B structural changes monitored by infrared spectroscopy, *J. Lipid Res. 42*, 778−782.
22. De Spirito, M., Brunelli, R., Mei, G., Bertani, F. R., Ciasca, G., Greco, G., Papi, M., Arcovito, G., Ursini, F., and Parasassi, T. (2006) Low density lipoprotein aged in plasma forms clusters resembling subendothelial droplets: aggregation via surface sites, *Biophys. J. 90*, 4239−4247.
23. Xu, S., and Lin, B. (2001) The mechanism of oxidation-induced low-density lipoprotein aggregation: an analogy to colloidal aggregation and beyond? *Biophys. J. 81*, 2403−2413.
24. Gallego-Nicasio, J., López-Rodríguez, G., Martínez, R., Tarancón, M. J., Fraile, V, M., and Carmona, P. (2003) Structural changes of low density lipoproteins with Cu^{2+} and glucose induced oxidation, *Biopolymers 72*, 514−520.
25. Jayaraman, S., Gantz, D. L., and Gursky, O. (2005) Structural basis for thermal stability of human low-density lipoprotein, *Biochemsitry 44*, 3965−3971.
26. Arnhold, J., Weigel, D., Richter, O., Hammerschmidt, S., Arnold, K., and Krumbiegel, M. (1991) Modification of low density lipoproteins by sodium hypochlorite, *Biomed. Biochim. Acta 50*, 967−973.
27. Schumaker, V. N., and Puppione, D. L. (1986) Sequential floatation ultracentrifugation. *Methods Enzymol. 128*, 155−170.
28. Pinchuk, I., Schnitzer, E., and Lichtenberg, D. (1998) Kinetic analysis of copper-induced peroxidation of LDL, *Biochim. Biophys. Acta 1389*, 155−172.
29. Hoff, H. F., Whitaker, T. E., and O'Neil, J. (1992) Oxidation of low density lipoprotein leads to particle aggregation and altered macrophage recognition, *J. Biol. Chem. 267*, 602−609.
30. Hazell, L. J., and Stocker, R. (1993) Oxidation of low-density lipoprotein with hypochlorite caused transformation of the lipoprotein into a high-uptake form for macrophages, *Biochem. J. 290*, 165−172.
31. Exner, M., Hermann, M., Hofbauer, R., Hartmann, B., Kapiotis, S., and Gmeiner, B. (2004) Thiocyanate catalyzes myeloperoxidase-initiated lipid oxidation in LDL, *Free Radical Biol. Med. 37*, 146−155.

32. Podrez, E. A., Schmitt, D., Hoff, H. F., and Hazen, S. L. (1999) Myeloperoxidase-generated reactive nitrogen species convert LDL into atherogenic form in vitro, *J. Clin. Invest. 103*, 1547−1560.
33. Benjwal, S., Verma, S., Röhm, K-H., and Gursky, O. (2006) Monitoring protein aggregation during thermal unfolding in circular dichroism experiments, *Protein Sci. 15*, 635−639.
34. Gursky, O., and Aleshkov, S. (2000) Temperature-dependent β-sheet formation in β-amyloid Aβ(1−40) peptide in water: uncoupling β-structure folding from aggregation, *Biochim. Biophys. Acta 1476*, 93−102.
35. Yang, W. Y., Larios, E., and Gruebele, M. (2003) On the extended beta-conformation propensity of polypeptides at high temperature, *J. Am. Chem. Soc. 125*, 16220−16227.
36. Sunde, M., and Blake, C. C. (1998) From the globular to the fibrous state: protein structure and structural conversion in amyloid formation, *Q. Rev. Biophys. 31*, 1−39.
37. Khurana, R., Coleman, C., Ionescu-Zanetti, C., Carter, S. A., Krishna, V., Grover, R. K., Roy, R., and Singh, S. (2005) Mechanism of thioflavin T binding to amyloid fibrils, *J. Struct. Biol. 151*, 229−238.
38. Khurana, R., Uversky, V. N., Nielsen, L., and Fink, A. L. (2001) Is Congo red an amyloid-specific dye? *J. Biol. Chem. 276*, 22715−22721.
39. Bottazzi, B., Vouret-Craviari, V., Bastone, A., De Gioia, L., Matteucci, C., Peri, G., Spreafico, F., Pausa, M., D'Ettorre, C., Gianazza, E., Tagliabue, A., Salmona, M., Tedesco, F., Introna, M., and Mantovani, A. (1997) Multimer formation and ligand recognition by the long pentraxin PTX3. Similarities and differences with the short pentraxins C-reactive protein and serum amyloid P component, *J. Biol. Chem. 272*, 32817−32823.
40. Li, X. A., Yutani, C., and Shimokado, K. (1998) Serum amyloid P component associates with high density lipoprotein as well as very low density lipoprotein but not with low density lipoprotein, *Biochem. Biophys. Res. Commun. 244*, 249−252.
41. Orlova, E. V., Sherman, M. B., Chiu, W., Mowri, H., Smith, L. C., and Gotto, A. M., Jr. (1999) Three-dimensional structure of low density lipoproteins by electron cryomicroscopy, *Proc. Natl. Acad. Sci. U.S.A. 96*, 8420−8425.
42. Mehta, R., Gantz, D. L., and Gursky, O. (2003) Human plasma high-density lipoproteins are stabilized by kinetic factors, *J. Mol. Biol. 328*, 183−192.
43. Jayaraman, S., Gantz, D. L., and Gursky, O. (2006) Effects of salt on the thermal stability of human plasma high-density lipoprotein, *Biochemistry 45*, 4620−4628.
44. Aggerbeck, L. P., Kezdy, F. J., and Scanu, A. M. (1976) Enzymatic probes of lipoprotein structure. Hydrolysis of human serum low density lipoprotein-2 by phospholipase A2, *J. Biol. Chem. 251*, 3823−3830.
45. Blumenthal, R., Clague, M. J., Durell, S. R., and Epand, R. M. (2003) Membrane fusion, *Chem. Rev. 103*, 53−69.
46. Pentikainen, M. O., Lehtonen, E. M., and Kovanen, P. T. (1996) Aggregation and fusion of modified low density lipoprotein, *J. Lipid Res. 37*, 2638−2649.
47. Pentikainen, M. O., Lehtonen, E. M., Oorni, K., Lusam, S., Somerharju, P., Jauhiainen, M., and Kovanen, P. T. (1997) Human arterial proteoglycans increase the rate of proteolytic fusion of low density lipoprotein particles, *J. Biol. Chem. 272*, 25283−25288.

BI700225A